



Published in final edited form as:

Cancer Immunol Res. 2015 March ; 3(3): 228–235. doi:10.1158/2326-6066.CIR-14-0001.

Peptide/MHC tetramer-based sorting of CD8⁺ T cells to a leukemia antigen yields clonotypes drawn nonspecifically from an underlying restricted repertoire

Sally A. Hunsucker^{1,†}, Colleen S. McGary^{1,†}, Benjamin G. Vincent^{1,†}, Atim A. Enyenihi², Jennifer P. Waugh³, Karen P. McKinnon¹, Lisa M. Bixby¹, Patricia A. Ropp¹, James M. Coghill^{1,3}, William A. Wood^{1,3}, Don A. Gabriel^{1,3}, Stefanie Sarantopoulos^{1,3}, Thomas C. Shea^{1,3}, Jonathan S. Serody^{1,3}, Gheath Alatrash⁴, Tania Rodriguez-Cruz⁵, Gregory Lizée⁵, Adam S. Buntzman⁶, Jeffrey A. Frelinger⁶, Gary L. Glish², and Paul M. Armistead^{1,3,*}

¹Lineberger Comprehensive Cancer Center, Chapel Hill, North Carolina

²Department of Chemistry, University of North Carolina, Chapel Hill, North Carolina

³Department of Medicine, University of North Carolina, Chapel Hill, North Carolina

⁴Section of Transplantation Immunology, Department of Stem Cell Transplant and Cellular Therapy

⁵Department of Melanoma, M.D. Anderson Cancer Center, Houston, Texas

⁶Department of Immunobiology, University of Arizona, Tucson, Arizona

Abstract

Testing of T cell-based cancer therapeutics often involves measuring cancer antigen-specific T-cell populations with the assumption that they arise from *in vivo* clonal expansion. This analysis, using peptide/MHC tetramers, is often ambiguous.

From a leukemia cell line, we identified a CDK4-derived peptide epitope, UNC-CDK4-1 (ALTPVVVTL) that bound HLA-A*02:01 with high affinity and could induce CD8⁺ T-cell responses *in vitro*. We identified UNC-CDK4-1/HLA-A*02:01 tetramer⁺ populations in 3 of 6 patients with acute myeloid leukemia who had undergone allogeneic stem cell transplant (SCT).

Using tetramer-based, single-cell sorting and T-cell receptor β (TCR β) sequencing we identified recurrent UNC-CDK4-1 tetramer-associated TCR β clonotypes in a patient with a UNC-CDK4-1 tetramer⁺ population, suggesting *in vivo* T-cell expansion to UNC-CDK4-1. In parallel, we measured the patient's TCR β repertoire and found it to be highly restricted / oligoclonal. The UNC-CDK4-1 tetramer-associated TCR β clonotypes represented >17% of the entire TCR β repertoire – far in excess of the UNC-CDK4-1 tetramer⁺ frequency, indicating that the recurrent TCR β clonotypes identified from UNC-CDK-4-1 tetramer⁺ cells were likely a consequence of the

Corresponding Author: Paul Michael Armistead, 450 West Drive, 21-244, Chapel Hill, NC 27599, Phone 919-843-6847, Fax 919-966-8212, Email paul_armistead@med.unc.edu.

[†]These authors contributed equally to this project

The authors have no relevant financial conflicts of interest.

extremely constrained T-cell repertoire in the patient and not *in vivo* UNC-CDK4-1-driven clonal T-cell expansion.

Mapping recurrent TCR β clonotype sequences onto TCR β repertoires can help confirm or refute antigen-specific T-cell expansion *in vivo*.

Keywords

T-cell repertoire; Single-cell T-cell receptor sequencing; Leukemia antigen; Tetramer analysis; Immune monitoring

Introduction

Part of measuring the efficacy of T cell-based therapies like cancer vaccines, adoptive T-cell therapies, and allogeneic stem cell transplantation (SCT) involves quantifying antigen-specific T-cell responses, which usually is accomplished using peptide/MHC tetramers (1-4). While the enumeration of tetramer⁺ cells is considered a measurement of antigen-specific T-cell expansion, this assumption may be invalid in the setting of low-frequency, or low affinity responses - as is often the case in the measurement of cancer antigen-specific T-cells.

Antigen-specific T-cell expansion should yield clonal populations with recurrent TCR β sequences in tetramer⁺ populations (5). In this report we describe the use of tetramer-based fluorescence activated cell sorting (FACS) to identify recurrent, potentially “antigen-specific” TCR β CDR3 sequences, i.e. TCR β clonotypes, which were then mapped onto a patient's TCR β CDR3 repertoire. By comparing the frequency of tetramer⁺ cells to the frequency of tetramer-associated TCR β CDR3 sequences in a patient's CD8⁺ T-cell repertoire we were able to support *in vivo* clonal T-cell expansion to a viral antigen (pp65_{NLV}) and refute clonal expansion to a potentially novel leukemia-associated antigen (UNC-CDK4-1, ALTPVVVTL) in an SCT patient *despite* detection of recurrent UNC-CDK4-1 tetramer-associated TCR β clonotypes.

Materials and Methods

Detailed descriptions are included in supplementary materials.

Identification of HLA-A*02:01 restricted peptides by HPLC-MS

A lysate of 6×10^9 HLA-A*02:01-transfected U937 cells (U937.A2) was cleared by ultracentrifugation, and the supernatant passed over a BB7.2-loaded HiTRAP recombinant protein A column. The BB7.2/HLA/peptide complexes were eluted with acetic acid, and the eluate passed through Microcon 3 K filters to yield peptide epitopes (6).

A Hitachi NanoFrontier Nano LC / linear ion trap time-of-flight mass spectrometer was used for online LC-MS/MS experiments. The peptide mixture was injected and subjected to data-dependent acquisition using collision-induced dissociation (CID) for peptide ion activation.

MS/MS ion searching was performed using the Mascot search engine, with the no enzyme option and non-identical protein database (NCBIInr).

Western blot analysis

Twenty μg each of 3 human AML PBMC lysates, a healthy donor PBMC lysate and a Jurkat cell lysate were electrophoresed on a 4-12% NuPAGE gradient gel and transferred to a PVDF membrane. CDK4 was detected with a primary antibody (Abcam, ab75511) followed by an HRP-conjugated anti-mouse antibody. Bands were visualized using Amersham ECL Western blotting reagents.

iTopia affinity and off-rate assays

Epitope binding was measured using the iTopia Epitope Discovery System. For binding affinity, peptides were incubated in HLA-A*02:01-coated wells overnight, in the presence of the anti-HLA antibody, and fluorescence was read on a Synergy 2 microplate reader with results compared to the binding of the positive control peptide (FLPSDFFPSV, from Hepatitis B core protein) at 10^{-4} M. The EC_{50} was determined using GraphPad Prism's nonlinear regression 'log (agonist) versus response – variable slope (four parameter)' curve. For the off-rate assay, peptides were incubated in HLA-A*02:01-coated wells at $11 \mu\text{M}$ overnight, then washed. Fluorescence was read at the times indicated on the graph. The $t_{1/2}$ was calculated using GraphPad Prism's nonlinear regression, 'dissociation – one phase exponential decay' curve.

UNC-CDK4-1-specific cytotoxic T-cell generation

Antigen-specific T cells were generated based on the method of Wöflfl and Greenberg with some modifications (7). HLA-A*02:01-expressing monocyte-derived DCs were generated following adherence to plastic and incubation with IL4 10 ng/mL and GM-CSF 800 IU with the addition of 10 ng/mL LPS, 100 IU/mL $\text{IFN}\gamma$ on the fifth day. The DCs were pulsed with $20 \mu\text{g/mL}$ UNC-CDK4-1 peptide and irradiated at 30 Gy . Naïve CD8^+ cells were isolated from the non-adherent fraction by negative selection using Miltenyi MACS beads with subsequent negative selection using anti-CD57 and anti-CD45RO beads. The naïve CD8^+ cells and peptide-pulsed DCs were co-incubated at a ratio of 4:1 with IL21 at 30 ng/mL . On day 3 of co-culture IL15 at 5 ng/mL and IL7 at 5 ng/mL were added. Cultures were analyzed on day 11.

CD107 / $\text{IFN}\gamma$ T-cell activation assay

Antigen-specific activity was measured by flow cytometry quantifying CD107 and $\text{IFN}\gamma$ expression described by Betts and colleagues (8). Autologous DCs were pulsed with $20 \mu\text{g/mL}$ of PR1 (VLQELNVTV) peptide, $20 \mu\text{g/mL}$ of UNC-CDK4-1, or left unpulsed. As a positive control, non-specific stimulation with phytohemagglutinin (PHA) was also performed. T cells were mixed with DCs at a 1:1 ratio and incubated with PE-labeled anti-CD107a, PE-labeled anti-CD107b and anti-CD28/49d. After 1 hour, the cells were treated with Brefeldin A and monensin. After incubation for an additional 5 hours, cells were washed, permeabilized and fixed. The cells were blocked with IgG and incubated with

PerCP-labeled anti-CD8 and FITC-labeled anti-IFN γ . After 30 minutes the cells were analyzed by flow cytometry.

Tetramer flow cytometry

PBMCs (5×10^5 to 1×10^6) from cryopreserved post-SCT AML patients were incubated in DPBS with Pacific Blue-conjugated CD4, CD14 CD16 and CD19 (lineage) antibodies, FITC-conjugated CD8 antibody, and PE-UNC-CDK4-1/HLA-A*02:01 tetramer at 4°C for 25 minutes. Live/Dead Fixable Far Red Stain was added and cells were incubated for 5 minutes at 4°C. Samples were washed and analyzed on a MACSQuant flow cytometer. Tetramer-positive cells were enumerated in the live (far red negative), lymphocyte (FSC/SSC), “lineage” (Pacific Blue) negative, CD8 (FITC) positive gate (9-11). A negative tetramer and/or a fluorescence minus one (FMO) sample was used to set the tetramer gate.

FACS Tetramer analysis and single-cell sorting

PBMCs from Patient 5 were stained with CD8-Pacific Orange along with PE-HLA-A*02:01 tetramers generated with CMV-pp65_{NLV} (NLVPMVATV), UNC-CDK4-1, and negative control peptides. For single-cell sorting, sort gates were determined by setting the CD8⁺ Tetramer⁺ gate so that it included no cells in the negative tetramer sample. Tetramer⁺CD8⁺ T cells were sorted by an iCyt Reflection high-speed sorter at 1 cell/well into a 96-well PCR plate each well containing 4 μ L buffer (0.5 \times PBS, 10 mM DTT, and 8 U RNaseOUT) (12). The same method was used for single-cell CD8⁺ sorting except no tetramers were used.

Single-cell PCR and sequencing

RT-PCR amplification and sequencing of TCR β clonotypes was performed using multiplex primers (Supplementary Table 1) and nested PCR covering all human TCR β variable region genes and the β -chain constant region (12). PCR products were treated with Exonuclease I and shrimp alkaline phosphatase and sequenced by the UNC Genome Analysis Facility. TCR β sequence identifications were made using the SoDA software tool (13). Tetramer-PE fluorescence vs. CD8-Pacific Orange fluorescence values were plotted for each T-cell's TCR β clonotype using an R script.

Bulk TCR β repertoire sequencing

PBMCs were isolated from a second sample from Patient 5 obtained 2 months after the initial sample. Bulk CD8⁺ T cells were sorted, and RNA was extracted from 3×10^6 CD8⁺ T cells using the RNEasy kit. The TCR β repertoire was amplified using a RT-PCR protocol and the iRepertoire multiplex primer set (14). The sequencing library was run using 2 \times 100 paired-end chemistry on an Illumina HiSeq 2000 sequencer in the UNC High Throughput Sequencing Facility.

High-throughput sequencing data analysis

Sequence data were processed using Python and R scripts developed in the lab. Paired-end reads were analyzed for the presence of the conserved invariant cysteine and FGXG motifs that define the CDR3 region in one reading frame. Sequences that did not exhibit this motif, had stop codons in the motif reading frame, or were present at less than three copies in the

dataset were excluded. V β and J β gene identifications were made by either exact alignment or the highest-scoring Smith-Waterman alignment to the germline reference gene sequences annotated in IMGT (<http://www.imgt.org/IMGTrepertoire>) (15, 16).

Results

In vitro analysis of the UNC-CDK4-1 antigen

By HPLC-tandem MS we identified 34 candidate leukemia-associated antigens (LAA) from U937.A2 cells (Supplementary Table 2) and focused on the CDK4-derived peptide ALTPVVVTL (Figure 1A) because CDK4 is a therapeutic target in leukemia (17-19). Western blotting confirmed CDK4 overexpression in human AML but not in normal PBMCs (Figure 1B). Using the iTopia assay, we measured an equilibrium EC₅₀ of 2.4 μ M for UNC-CDK4-1 and a dissociation t_{1/2} > 8 hr, the longest time point in the assay, (Figure 1C, 1D).

Using UNC-CDK4-1-pulsed autologous dendritic cells as stimulators we generated a T-cell product that showed antigen-specific killing against UNC-CDK4-1 (Figure 1E-H), and in experiments using UNC-CDK4-1-pulsed T2 cells as stimulators, we generated a T-cell population with 0.2% of CD8⁺ cells specific for UNC-CDK4-1 (Supplementary Figure 1).

Measurements of UNC-CDK4-1 T-cell responses in post-SCT patients

PE-UNC-CDK4-1/HLA-A*02:01 tetramers were used to probe for UNC-CDK4-1-specific T-cell responses in 6 HLA-A*02:01-expressing, post-SCT, AML patients (Table 1). Based on *in vitro* expansion experiments, we set a threshold for a tetramer⁺ population of >0.01% as *possibly* representing a UNC-CDK4-1-specific T-cell response. We observed UNC-CDK4-1/HLA-A*02:01 tetramer frequencies of >0.01% of CD8⁺ cells in 3 of the 6 patients (Figure 2A-F, Supplementary Figure 2), but all frequencies were low, raising the possibility that the identified cells did not represent a true antigen-specific response.

Antigen-specific T-cell responses generate clonally expanded T-cell populations with the same TCR β clonotypes (5). We performed tetramer-based single-cell sorting with TCR β CDR3 sequencing on a PBMC sample from Patient 5 (Figure 2E) using tetramers specific to UNC-CDK4-1 or the CMV pp65_{NLV} epitope. The patient and donor were CMV seropositive pre-SCT. The patient had developed CMV viremia 2 months post-SCT, but he was not viremic at the time of this sample collection. There were 5 recurrent TCR β clonotypes in the pp65_{NLV}-tetramer⁺ sorted cells and 6 recurrent TCR β clonotypes in the UNC-CDK4-1-tetramer⁺ cells (Figure 2G-J, Supplementary Table 3). The cells in each recurrent clonotype had the same nucleic acid and amino acid CDR3 sequence. For the pp65_{NLV} tetramer⁺ cells the TCR β clonotype containing epitope ASRPFVNTEA had significantly higher tetramer affinity compared to the next 2 most prevalent pp65_{NLV}-specific TCR β clonotypes (Figure 2I); however, no UNC-CDK4-1-specific TCR β clonotype showed a statistically significant higher affinity (Figure 2J).

Tetramer-associated TCR β clonotypes map to the TCR β repertoire at different frequencies

Using a 2-month subsequent sample from Patient 5, we measured the frequency of the tetramer-associated TCR β clonotypes (Figure 2G-J) in the patient's CD8⁺ TCR β repertoire. After removing sequences supported by 2 reads as possible sources of PCR or sequencing errors, our TCR β repertoire contained 1.02×10^8 reads with 9.5×10^7 yielding functional TCR β sequences. The frequency of different V β and J β combinations varied greatly (Figure 3A). Furthermore, the diversity of CDR3 region amino acid lengths (analogous to TCR β spectratyping) showed a non-parametric distribution suggesting a highly constrained/oligoclonal TCR β repertoire (Figure 3B, Supplementary Table 4) (20-22).

We graphed the 5,043 unique clonotypes according to their frequency in the dataset. The clonotype frequencies varied from 1 clonotype (V6-5_J1-1_ASWTGEGNTEA) representing 0.28 (28%) of the repertoire to 1,346 unique clonotypes each having the minimum clonotype frequency (supported by 3 reads in the repertoire) of 3.16×10^{-8} . All 6 UNC-CDK4-1 tetramer⁺ associated TCR β clonotypes were present at unexpectedly high frequencies from 0.038% to 12%, while the three pp65_{NLV} tetramer⁺ associated TCR β clonotypes identified in the repertoire were present at between 0.00011% to 0.0016% (Figure 3C). To test for amplification bias in the repertoire analysis we obtained another sample from Patient 5, 6 months after the sample used for repertoire analysis, and performed single-cell sorting of CD8⁺ cells with TCR β CDR3 sequencing. From 95 sorted CD8⁺ cells we obtained 86 TCR β CDR3 sequences. All 6 recurrent UNC-CDK4-1 tetramer⁺ associated clonotypes were again present at extremely high frequencies (Figure 3D). By comparing frequency of the UNC-CDK4-1 and pp65_{NLV}-associated TCR β clonotypes in their respective tetramer⁺ gates (Figures 2G and 2H) to their frequencies in the repertoire (Figure 3C) we measured an enrichment ratio for each clonotype, i.e. clonotype frequency in tetramer⁺ gate / clonotype frequency in bulk repertoire (Figure 3E). The mean enrichment ratio for the pp65_{NLV}-associated clonotypes was 7.63×10^5 , while the mean enrichment for the UNC-CDK4-1 was only 1.04×10^1 .

Discussion

Peptide/MHC tetramers are often used to measure antigen-specific T-cell responses *in vivo*; however, the data they provide can be ambiguous. As part of an antigen discovery project, we identified UNC-CDK4-1 as a potential LAA. CDK4 is overexpressed in AML, the UNC-CDK4-1 epitope has high affinity to HLA-A*02:01 (23), and tolerance to UNC-CDK4-1 can be broken. Based on these *in vitro* data, we tested for UNC-CDK4-1 responses *in vivo*.

Using UNC-CDK4-1/HLA-A*02:01 tetramers we identified tetramer⁺ T cells at a frequency of > 0.01%, higher than our sensitivity cut-off, in 3 of 6 post-SCT AML patients. The tetramer results were ambiguous because of the low number of tetramer⁺ cells and many of the gated CD8⁺ T cells had low affinity for the tetramer. To address this ambiguity, we performed tetramer-based single-cell sorting and TCR β CDR3 sequencing to test for recurrent TCR β clonotypes (5).

We isolated UNC-CDK4-1 and pp65_{NLV} tetramer⁺ T cells from Patient 5 and identified tetramer-associated recurrent TCR β clonotypes. While recurrent TCR β clonotypes identified

in a tetramer-defined population typically confirms the discovery of antigen-specific T-cell clonal populations (5), our repertoire mapping studies show that this is not the case in all situations.

Tetramer analysis of Patient 5's T cells identified a rare T-cell population (0.04%) recognizing UNC-CDK4-1; however, the recurrent UNC-CDK4-1-associated TCR β clonotypes represented ~15% of the patient's CD8⁺ repertoire. In contrast, the patient had a T-cell population (**0.07%**, Supplementary Figure 2) recognizing the pp65_{NLV} antigen and the recurrent pp65_{NLV}-associated TCR β clonotypes only represented 0.002% of the patient's TCR β repertoire. The low frequency of pp65_{NLV} tetramer⁺ cells are consistent with antigen-specific memory T cells in a CMV-exposed but not viremic subject, like this patient. While the differences in clonotype frequency measured by tetramer compared to TCR β repertoire analysis for pp65_{NLV}-associated clonotypes could be explained by the 2 month difference in sample collection dates, tetramer gating and TCR repertoire sampling, it is unlikely that these factors explain the vast differences observed in the UNC-CDK4-1-associated clonotypes. By measuring the frequency of TCR β clonotypes in a tetramer⁺ sample and in the bulk T-cell repertoire, we demonstrated that the pp65_{NLV}-associated clonotypes were highly enriched in their tetramer⁺ gate, while the UNC-CDK4-1-associated clonotypes were not – suggesting that the recurrent UNC-CDK4-1-associated clonotypes are not antigen-specific whereas the pp65_{NLV} associated clonotypes are antigen-specific (Figure 3E).

Overexpression of TCRs in some cells or preferential amplification of specific TCR β CDR3 regions could affect TCR β repertoire analysis. However, the primers used in the TCR β CDR3 repertoire analysis minimize amplification bias (14), and our single-cell CD8⁺ TCR β CDR3 sequencing reports the TCR β clonotype for individual cells. Because the frequencies between the repertoire and CD8⁺ single-cell analysis are so similar (Figure 3C-D) the highly restricted repertoire observed is likely an accurate representation of Patient 5's T-cell repertoire.

Our study did not analyze TCR α sequences, and while it is conceivable that the highly prevalent TCR β sequences found in Patient 5 could be paired with multiple different TCR α sequences this phenomenon is unlikely given the mechanism behind TCR assembly and has not, to our knowledge, been described (5, 24, 25).

In this patient's highly restricted (i.e. oligoclonal) T-cell repertoire, which is common in patients following SCT (21, 22), the majority of T cells identified in the UNC-CDK4-1 tetramer⁺ gate are derived from the expanded pools of T cells that are not antigen-specific. Tetramer-based TCR β clonotype analysis in a highly restricted T-cell repertoire can lead to clonotypically identical T cells stochastically being captured in a tetramer⁺ gate and misinterpreted as antigen-specific. This potential error can be addressed by TCR β repertoire mapping.

Supplementary Material

Refer to Web version on PubMed Central for supplementary material.

Acknowledgements and Authorship

S.A.H. designed and conducted experiments and edited the manuscript. C.M. designed and conducted experiments. B.G.V. designed and conducted experiments and edited the manuscript. A.A.E. designed and conducted experiments. J.P.W. designed and conducted experiments. L.M.B. designed and conducted experiments. K.P.M. designed and conducted experiments. P.A.R. designed and conducted experiments. J.M.C, W.A.W, D.A.G, S.S and T.C.S enrolled patients for analysis. J.S.S. enrolled patients for analysis and edited the manuscript. G.A. designed experiments and edited the manuscript. T.R-C. contributed U937-A2 cells. G.L contributed U937-A2 cells. A.S.B. designed experiments and edited the manuscript. J.A.F. designed experiments and edited the manuscript. G.L.G. designed experiments and edited the manuscript. P.M.A designed and conducted experiments and wrote the manuscript.

Support: BGV received salary support through T32 HL007149-37. PMA received salary support through KL2 TR000084 and K08 HL113594-01.

References

1. Chapuis AG, Ragnarsson GB, Nguyen HN, Chaney CN, Pufnock JS, Schmitt TM, et al. Transferred WT1-reactive CD8+ T cells can mediate antileukemic activity and persist in post-transplant patients. *Sci Transl Med.* 2013; 5:174r. a27.
2. Greiner J, Schmitt A, Giannopoulos K, Rojewski MT, Gotz M, Funk I, et al. High-dose RHAMM-R3 peptide vaccination for patients with acute myeloid leukemia, myelodysplastic syndrome and multiple myeloma. *Haematologica.* 2010; 95:1191–7. [PubMed: 20081055]
3. Meij P, Jedema I, van der Hoorn MA, Bongaerts R, Cox L, Wafelman AR, et al. Generation and administration of HA-1-specific T-cell lines for the treatment of patients with relapsed leukemia after allogeneic stem cell transplantation: a pilot study. *Haematologica.* 2012; 97:1205–8. [PubMed: 22511490]
4. Mollrem JJ, Lee PP, Wang C, Felio K, Kantarjian HM, Champlin RE, Davis MM. Evidence that specific T lymphocytes may participate in the elimination of chronic myelogenous leukemia. *Nat Med.* 2000; 6:1018–23. [PubMed: 10973322]
5. Wang GC, Dash P, McCullers JA, Doherty PC, Thomas PG. T cell receptor alphabeta diversity inversely correlates with pathogen-specific antibody levels in human cytomegalovirus infection. *Sci Transl Med.* 2012; 4:128ra42.
6. Hunt DF, Henderson RA, Shabanowitz J, Sakaguchi K, Michel H, Sevilir N, et al. Characterization of peptides bound to the class I MHC molecule HLA-A2.1 by mass spectrometry. *Science.* 1992; 255:1261–3. [PubMed: 1546328]
7. Wolf M, Greenberg PD. Antigen-specific activation and cytokine-facilitated expansion of naive, human CD8+ T cells. *Nat Protoc.* 2014; 9:950–66. [PubMed: 24675735]
8. Betts MR, Brenchley JM, Price DA, De Rosa SC, Douek DC, Roederer M, Koup RA. Sensitive and viable identification of antigen-specific CD8+ T cells by a flow cytometric assay for degranulation. *J Immunol Methods.* 2003; 281:65–78. [PubMed: 14580882]
9. Altman JD, Moss PA, Goulder PJ, Barouch DH, McHeyzer-Williams MG, Bell JI, et al. Phenotypic analysis of antigen-specific T lymphocytes. *Science.* 1996; 274:94–6. [PubMed: 8810254]
10. Armistead PM, Liang S, Li H, Lu S, Van Bergen CA, Alatrash G, et al. Common minor histocompatibility antigen discovery based upon patient clinical outcomes and genomic data. *PLoS One.* 2011; 6:e23217. [PubMed: 21858034]
11. Zhang M, Sukhumalchandra P, Enyenihi AA, St John LS, Hunsucker SA, Mittendorf EA, et al. A Novel HLA-A*0201 Restricted Peptide Derived from Cathepsin G Is an Effective Immunotherapeutic Target in Acute Myeloid Leukemia. *Clin Cancer Res.* 2013; 19:247–57. [PubMed: 23147993]
12. Vincent BG, Young EF, Buntzman AS, Stevens R, Kepler TB, Tisch RM, et al. Toxin-coupled MHC class I tetramers can specifically ablate autoreactive CD8+ T cells and delay diabetes in nonobese diabetic mice. *J Immunol.* 2010; 184:4196–204. [PubMed: 20220085]
13. Volpe JM, Cowell LG, Kepler TB. SoDA: implementation of a 3D alignment algorithm for inference of antigen receptor recombinations. *Bioinformatics.* 2006; 22:438–44. [PubMed: 16357034]

14. Wang C, Sanders CM, Yang Q, Schroeder HW Jr, Wang E, Babrzadeh F, et al. High throughput sequencing reveals a complex pattern of dynamic interrelationships among human T cell subsets. *Proc Natl Acad Sci U S A*. 2010; 107:1518–23. [PubMed: 20080641]
15. Lefranc MP, Giudicelli V, Ginestoux C, Jabado-Michaloud J, Folch G, Bellahcene F, et al. IMGT, the international ImMunoGeneTics information system. *Nuc Acids Res*. 2009; 37(Database issue):D1006–12.
16. Smith TF, Waterman MS. Identification of common molecular subsequences. *J Mol Biol*. 1981; 147:195–7. [PubMed: 7265238]
17. Karp JE, Smith BD, Resar LS, Greer JM, Blackford A, Zhao M, et al. Phase 1 and pharmacokinetic study of bolus-infusion flavopiridol followed by cytosine arabinoside and mitoxantrone for acute leukemias. *Blood*. 2011; 117:3302–10. [PubMed: 21239698]
18. Lin TS, Ruppert AS, Johnson AJ, Fischer B, Heerema NA, Andritsos LA, et al. Phase II study of flavopiridol in relapsed chronic lymphocytic leukemia demonstrating high response rates in genetically high-risk disease. *J Clin Oncol*. 2009; 27:6012–8. [PubMed: 19826119]
19. Malumbres M, Barbacid M. Cell cycle, CDKs and cancer: a changing paradigm. *Nat Rev Cancer*. 2009; 9:153–66. [PubMed: 19238148]
20. Krell PF, Reuther S, Fischer U, Keller T, Weber S, Gombert M, et al. Next-generation-sequencing-spectratyping reveals public T-cell receptor repertoires in pediatric very severe aplastic anemia and identifies a beta chain CDR3 sequence associated with hepatitis-induced pathogenesis. *Haematologica*. 2013; 98:1388–96. [PubMed: 23716544]
21. Liu C, He M, Rooney B, Kepler TB, Chao NJ. Longitudinal analysis of T-cell receptor variable beta chain repertoire in patients with acute graft-versus-host disease after allogeneic stem cell transplantation. *Biol Blood Marrow Transplant*. 2006; 12:335–45. [PubMed: 16503503]
22. van Heijst JW, Ceberio I, Lipuma LB, Samilo DW, Wasilewski GD, Gonzales AM, et al. Quantitative assessment of T cell repertoire recovery after hematopoietic stem cell transplantation. *Nat Med*. 2013; 19:372–7. [PubMed: 23435170]
23. Engels B, Engelhard VH, Sidney J, Sette A, Binder DC, Liu RB, et al. Relapse or eradication of cancer is predicted by peptide-major histocompatibility complex affinity. *Cancer Cell*. 2013; 23:516–26. [PubMed: 23597565]
24. Han A, Glanville J, Hansmann L, Davis MM. Linking T-cell receptor sequence to functional phenotype at the single-cell level. *Nat Biotechnol*. 2014; 32:684–92. [PubMed: 24952902]
25. Kim SM, Bhonsle L, Besgen P, Nickel J, Backes A, Held K, et al. Analysis of the paired TCR alpha- and beta-chains of single human T cells. *PLoS One*. 2012; 7:e37338. [PubMed: 22649519]

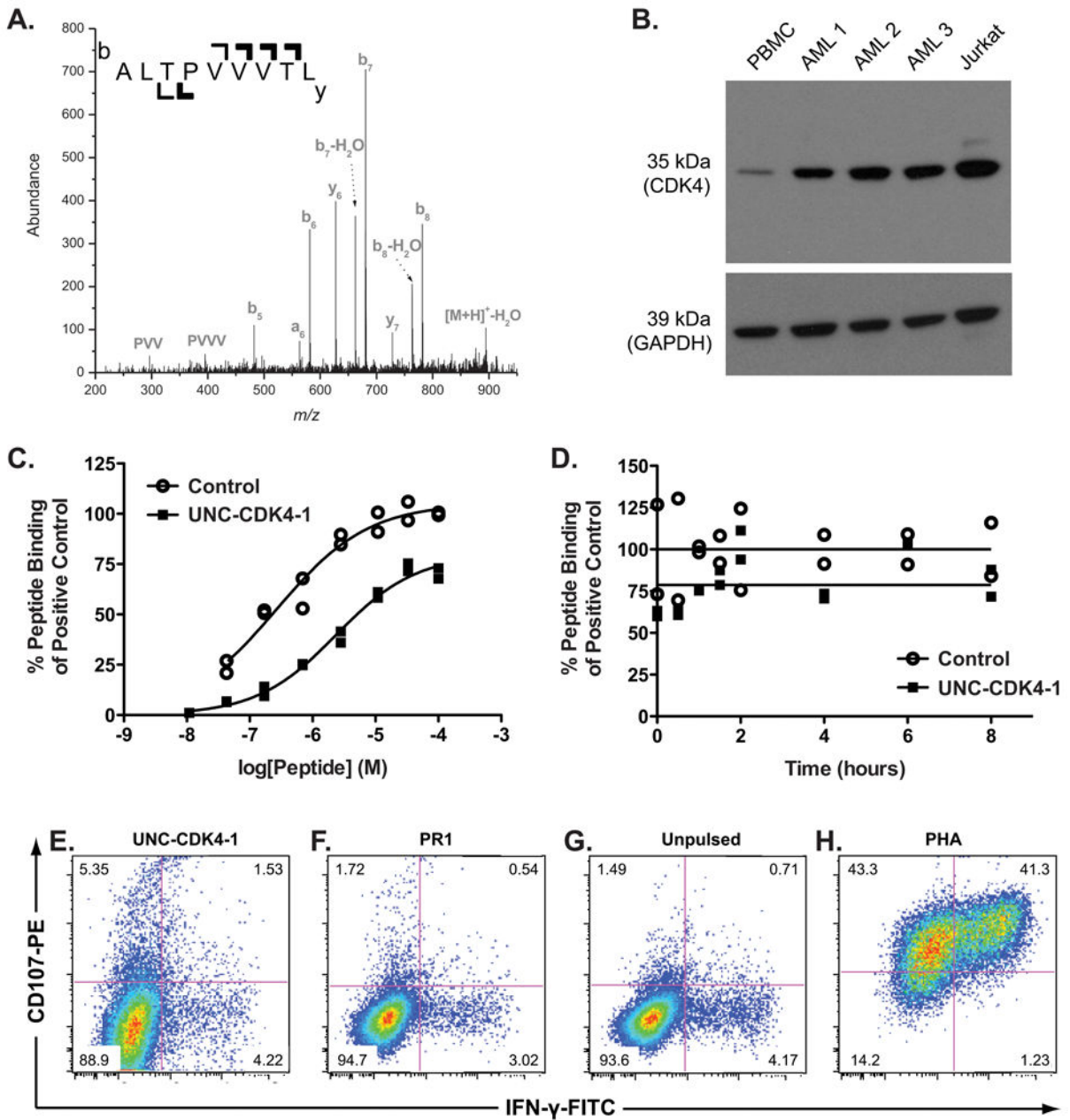


Figure 1. *In vitro* characterization of UNC-CDK4-1

(A) The tandem mass spectrum from the UNC-CDK4-1 peptide that was eluted from HLA-A*02:01-transfected U937 cells is shown. The singly charged peptide $[\text{M}+\text{H}]^+\text{-H}_2\text{O} = 894.56$ was identified. The b-ion series and y-ions, where b and y refer to N-terminal and C-terminal product ions respectively via peptide ion fragmentation nomenclature, uniquely matched to the CDK4 protein. (B) Western blot of CDK4 in whole-cell lysates from a healthy donor's PBMCs, 3 human AML samples, and the Jurkat cell line (positive control) are shown. CDK4 expression is significantly higher in all AML samples compared to that in healthy-donor PBMCs. (C) The concentrations to generate peptide/HLA complexes for UNC-CDK4-1 and control peptide (FLPSDFFPSV) with HLA-A*02:01 are shown. The

EC₅₀ of UNC-CDK4-1 binding to HLA-A*02:01 was measured using the iTopia assay and found to be 2.4 μM. **(D)** Complexes of UNC-CDK4-1/HLA-A*02:01 or FLPSDFFPSV/HLA-A*02:01 were assembled in multiple wells on the iTopia plates and non-bound peptide was washed away. At the given time points, the amount of peptide/HLA complex was measured and compared to the amount of peptide/HLA complex at t=0. The dissociation t_{1/2} of UNC-CDK4-1 from HLA-A*02:01, measured using the iTopia assay, is > 8 hr. Healthy donor T cells that had been co-cultured with UNC-CDL4-1-pulsed autologous DCs were tested for specific activity by measuring CD107 and IFNγ expression when stimulated by **(E)** autologous DCs pulsed with UNC-CDK4-1, **(F)** autologous DCs pulsed with PR1 antigen, **(G)** unpulsed autologous DCs. **(H)** non-specific stimulation with PHA as a positive control.

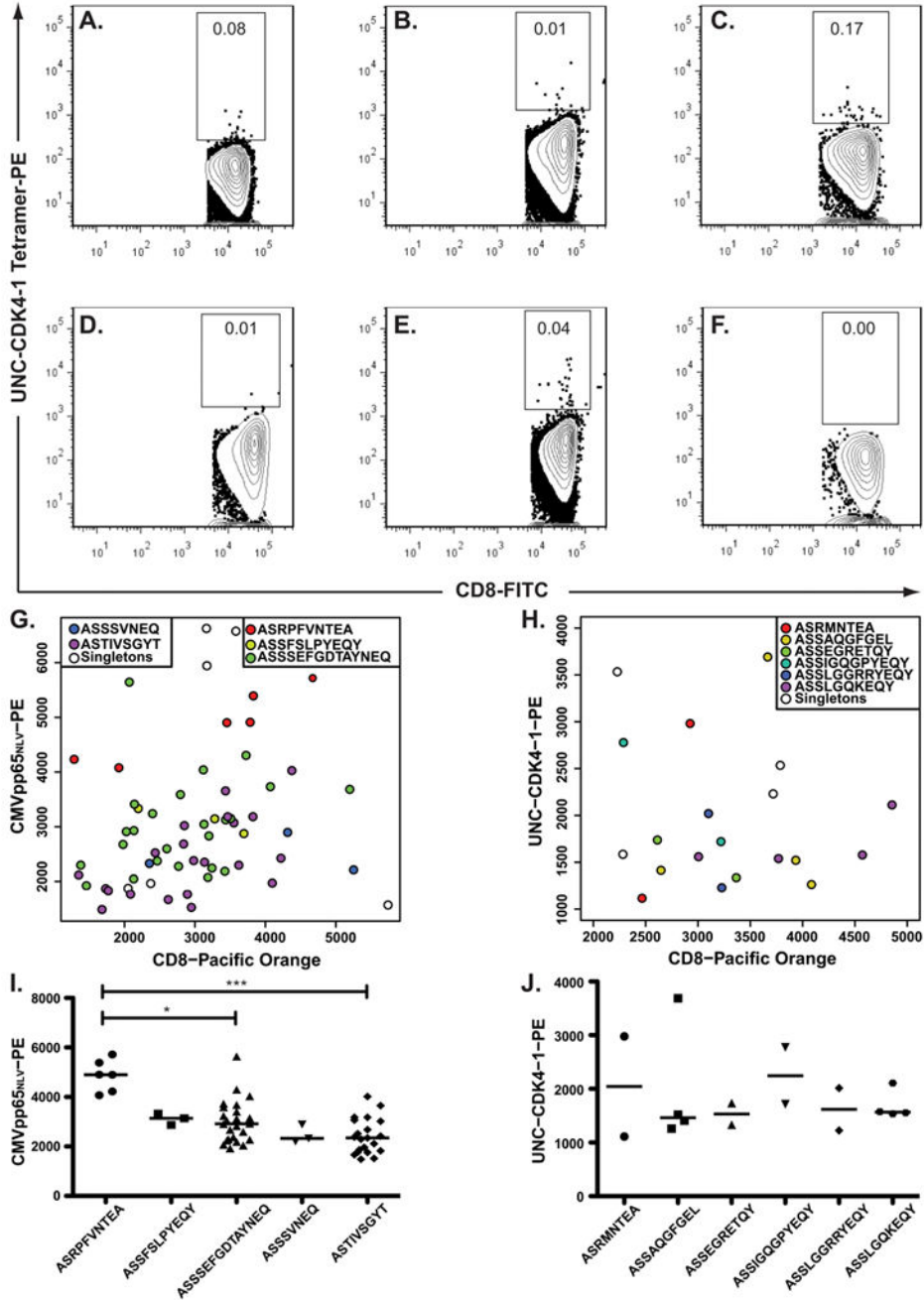


Figure 2. UNC-CDK4-1-specific CD8⁺ cells are expanded in AML patients post-SCT
 (A-F) 6 HLA-A*02:01-expressing AML patients who underwent SCT were evaluated for expanded populations of UNC-CDK4-1-specific CD8⁺ cells using UNC-CDK4-1 peptide-loaded tetramers. Because of the prior tissue culture studies, a tetramer⁺ value of > 0.01% was considered suggestive of an expanded UNC-CDK4-1-specific T-cell response. CD8⁺ cells from Patient 5 (2E) that were reactive to either pp65_{NLV} or UNC-CDK4-1 tetramers were individually sorted into wells of a 96-well plate, and their TCRβ V-CDR3-J sequences (i.e. clonotypes) were determined using RT-PCR followed by Sanger sequencing. The TCRβ

clonotype sequence from each well was indexed back to the fluorescence measurements obtained during the sort. The recurrent TCR β clonotypes reactive to **(G)** pp65_{NLV} or **(H)** UNC-CDK4-1 are shown as color-coded circles on the fluorescence graphs, and cells that have a unique TCR β clonotype are shown as unfilled circles. Comparisons of tetramer affinity among clonotypes were performed using an unpaired student t-test. **(I)** Clonotype ASRPFVNTEAF had significantly higher apparent avidity than the 2 most prevalent other pp65_{NLV} clonotypes (* P<0.05, *** P<0.01). Comparisons to the other pp65_{NLV}-reactive clonotypes could not be made because of low cell numbers. **(J)** No significant differences in tetramer affinity were measured in the UNC-CDK4-1 tetramer-associated clonotypes.

Author Manuscript

Author Manuscript

Author Manuscript

Author Manuscript

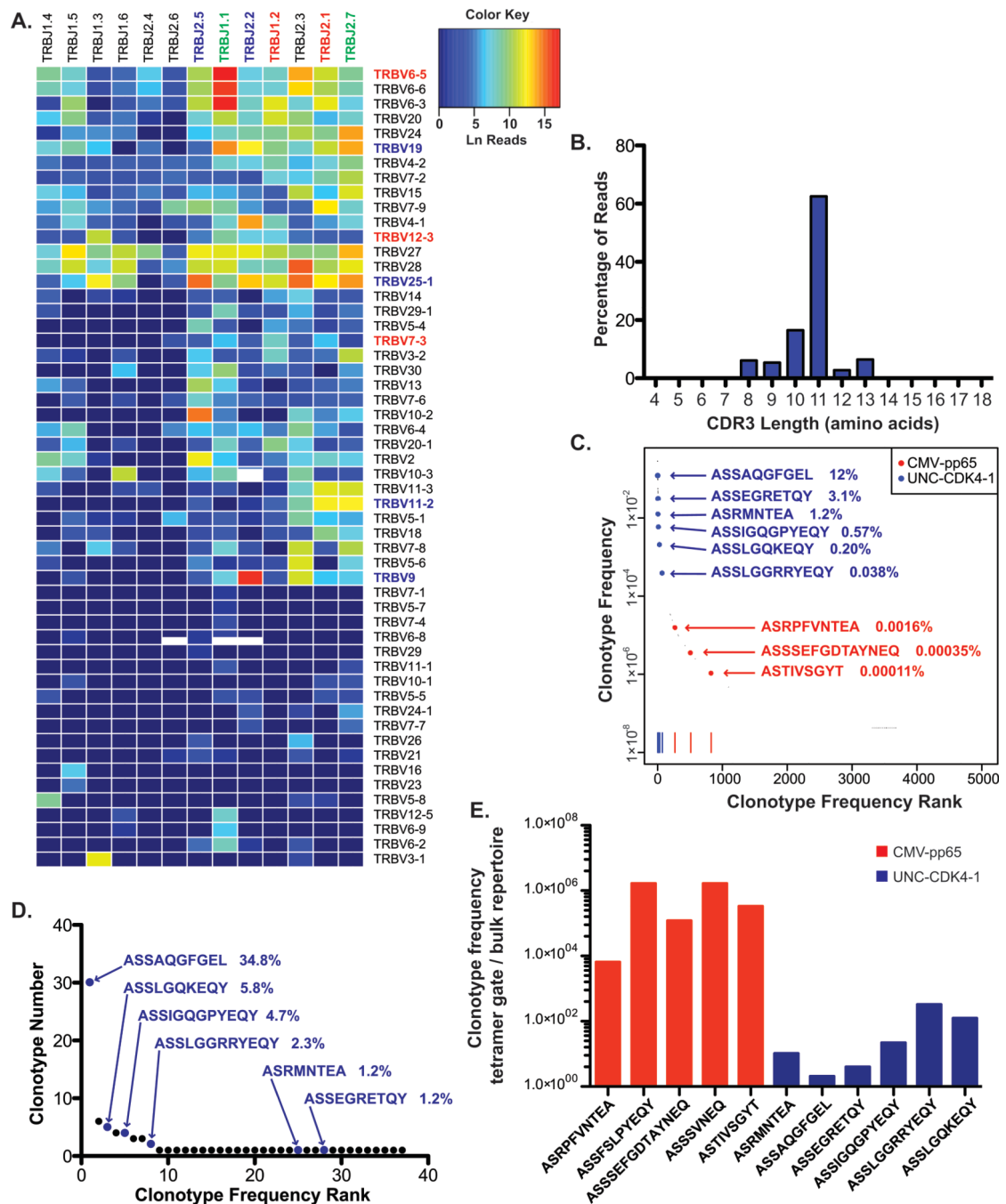


Figure 3. Antigen-specific TCRβ clonotypes map to the TCRβ repertoire at markedly different frequencies

3×10^6 CD8⁺ cells obtained from Patient 5 two months after the initial analytical tetramer study were analyzed for Vβ-Jβ distribution using the Illumina Hiseq platform. (A) The distribution of Vβ-Jβ combinations from the patient is shown. Vβ and Jβ families that were used in the antigen-specific TCRβ clonotypes are shown in blue (UNC-CDK4-1-associated), red (pp65_{NLV}-associated) or green (used in both antigen responses). (B) The reads that yielded functional TCRβ CDR3 regions were arranged by predicted CDR3 amino acid

length (starting from the amino acid immediately following the N-terminal invariant cysteine and ending immediately before the C-terminal invariant phenylalanine). The TCR β CDR3 repertoire was highly restricted with 78.99% of CR3 regions being either 10 or 11 amino acids in length. **(C)** The 5,043 determined TCR β clonotypes are ranked by decreasing clonotype frequency from left to right in the graph. 9 of the 11 TCR β clonotypes associated with either the pp65_{NLV} or UNC-CDK4-1 tetramer (Figure 2, Supplementary Table 4) are mapped onto the graph. Three of the 5 pp65_{NLV} tetramer-associated TCR β clonotypes (denoted in red) mapped to the TCR β repertoire with a frequency of 0.002% of the repertoire. In contrast, the 6 UNC-CDK4-1 tetramer-associated TCR β clonotypes (denoted in blue) represented 17.1% of the TCR β repertoire. **(D)** A 6-month follow-up sample from Patient 5 was analyzed using single-cell sorting of CD8⁺ cells and TCR β V-CDR3-J sequencing. All 6 UNC-CDK4-1 tetramer-associated TCR β clonotypes were identified at high frequencies in the 89 cells whose TCR β clonotype was determined. **(E)** The ratio of the frequencies of the TCR β clonotypes measured by single-cell tetramer sorting and bulk TCR β repertoire analysis are shown. UNC-CDK4-1-associated clonotypes are shown in blue, and pp65_{NLV}-associated clonotypes are shown in red. The bulk repertoire frequencies for pp65_{NLV}-associated clonotypes ASSFSLPYEQY and ASSSVNEQ that were not identified in the repertoire analysis were assigned the minimal frequency in the repertoire of 3.16×10^{-8} , the frequency of 1 copy in the repertoire. There was a statistically significant difference in the enrichment of pp65_{NLV}-associated (red) clonotypes in their tetramer⁺ gate compared to enrichment in the tetramer⁺ gate for the UNC-CDK4-1-associated clonotypes (blue) (t-test, $p < 0.0001$).

Table 1

Patient Characteristics.

Patient	Age	Gender	Disease	Collection day post-SCT	Absolute lymphocyte count ($\times 10^9/L$)	GVHD at collection	Systemic steroids at collection	GVHD prior to collection	Status
1	57	M	MDS / AML	+83	0.6	No	No	No	Alive (censored at day +1,085)
2	64	M	FLT3-ITD mutated AML	+164	0.7	Yes	Prednisone 2.5 mg daily	Acute grade II skin	Died of AML relapse at day +338
3	60	F	Relapsed AML	+368	0.9	Yes	No	Acute grade II skin Extensive chronic ocular, oral	Alive (censored at day +1,907)
4	60	F	Relapsed AML	+481	2.6	Yes	Prednisone 2.5 mg daily	Acute grade II skin Extensive chronic ocular, oral, cutaneous	Died of AML relapse at day +1,042
5	47	M	MF / AML	+567	5.7	No	No	Acute grade II skin	Alive (censored at day +1,446)
6	55	F	Treatment related AML	+569	1.2	No	No	No	Alive (censored at day +2,045)

Six HLA-A*02:01-expressing AML patients underwent allogeneic SCT at the North Carolina Cancer Hospital. Post-SCT samples were obtained at the post-SCT day of collection shown in column 5, and the absolute lymphocyte count at the time of collection is recorded in column 6. The presence of GVHD at the time of collection is listed in column 7, and systemic steroid use at the time of collection is shown in column 8. GVHD prior to sample collection is shown in column 9, and the long-term status of all 6 patients is shown in column 10.